

# HMOE: Hypernetwork-based Mixture of Experts for Domain Generalization

Jingang Qu<sup>1</sup> Thibault Faney<sup>2</sup> Ze Wang<sup>1</sup> Patrick Gallinari<sup>1,3</sup>  
 Soleiman Yousef<sup>2</sup> Jean-Charles de Hemptinne<sup>2</sup>

Sorbonne Université, CNRS, ISIR, 75005 Paris, France<sup>1</sup> IFPEN<sup>2</sup> Criteo AI Lab, Paris, France<sup>3</sup>

## Abstract

*Due to domain shifts, machine learning systems typically struggle to generalize well to new domains that differ from those of training data, which is what domain generalization (DG) aims to address. Although a variety of DG methods have been proposed, most of them fall short in interpretability and require domain labels, which are not available in many real-world scenarios. This paper presents a novel DG method, called HMOE: Hypernetwork-based Mixture of Experts (MoE), which does not rely on domain labels and is more interpretable. MoE proves effective in identifying heterogeneous patterns in data. For the DG problem, heterogeneity arises exactly from domain shifts. HMOE employs hypernetworks taking vectors as input to generate the weights of experts, which promotes knowledge sharing among experts and enables the exploration of their similarities in a low-dimensional vector space. We benchmark HMOE against other DG methods under a fair evaluation framework – DomainBed. Our extensive experiments show that HMOE can effectively separate mixed-domain data into distinct clusters that are surprisingly more consistent with human intuition than original domain labels. Using self-learned domain information, HMOE achieves state-of-the-art results on most datasets and significantly surpasses other DG methods in average accuracy across all datasets.*

## 1. Introduction

Domain generalization (DG) aims to train models on known domains to perform well on unseen domains, which is crucial for deploying models in safety-critical applications. Over the past decade, a variety of DG algorithms have been proposed [28, 87, 101], focusing primarily on developing DG-specific data augmentation techniques and learning domain-invariant representations to build generalizable predictors. However, many high-performing DG algorithms rely on domain labels to explicitly reduce inter-domain differences, severely limiting their applicability in real-world

scenarios where domain annotation may be prohibitively expensive. Additionally, current DG algorithms lack interpretability and cannot provide insight into the causes of success or failure in generalizing to new domains. Therefore, this work aims to develop a novel DG algorithm that does not require domain labels and is more interpretable.

We follow the nomenclature established by [11], which refers to DG with domain labels as vanilla DG and the more challenging DG without domain labels as compound DG. This work focuses on addressing compound DG by inferring latent domains from mixed-domain data and using them effectively. [6, 14, 58] demonstrated that using domain-wise datasets can theoretically yield lower generalization error bounds and better DG performance compared to using mixed data directly, indicating the importance of domain information. Furthermore, latent domain discovery helps us understand the workings of models and enhances interpretability. To make the problem tractable, we assume that latent domains are distinct and separable.

In this paper, we introduce HMOE: Hypernetwork-based Mixture of Experts (**MoE**). MoE is a well-established learning paradigm that aggregates a number of experts by calculating the weighted sum of their predictions [36, 37], where the aggregation weights, commonly referred to as gate values, are determined by a routing mechanism and add up to 1. HMOE capitalizes on MoE’s *divide and conquer* property, that is, the routing mechanism can softly partition the input space into subspaces in an unsupervised manner during training [92], with each subspace assigned to an expert. We further expect that each subspace is associated with a latent domain, enabling latent domain discovery. During inference, we can compare the similarities between an unseen test domain and the inferred domains based on gate values, hence improving interpretability. [29, 97] have validated MoE in domain adaptation [88] and showed that MoE can leverage the specialty of individual domain and alleviate negative knowledge transfer [75] compared to using a single model to learn different domains concurrently.

HMOE innovatively uses a neural network, called hypernetwork [30], which takes vectors as input to generate the weights for MoE’s experts. By mapping vectors to experts,

hypernetworks enable the exploration of experts' similarities in a low-dimensional vector space, facilitating latent domain discovery. Hypernetworks also serve as a bridge between experts and provide them a channel to exchange information, thereby promoting knowledge sharing.

MoE's intrinsic soft partitioning is not always effective and sometimes fails to maintain a consistent data division, especially when the distinction between latent domains is not significant. To address this issue, we propose a differentiable dense-to-sparse Top-1 routing algorithm, which forces gate values to become one-hot and converges to hard partitioning. This leads to sparse-gated MoE, which improves and stabilizes latent domain discovery. In addition, to better incorporate hypernetworks into MoE, we introduce an embedding space that contains a set of learnable embedding vectors corresponding one-to-one with experts. This embedding space is fed to hypernetworks to generate the weights of experts and is also part of the routing mechanism to compute gate values, thus enhancing the interaction between hypernetworks and the routing mechanism.

We also propose an intra-domain *mixup* to further improve the generalization ability of HMOE. *mixup* creates virtual training samples by taking a linear combination of two randomly chosen inputs and their labels [93], and we perform *mixup* within each inferred latent domain.

Our contributions are as follows: (1) We present a novel DG method – HMOE within the framework of MoE, that does not require domain labels, enables latent domain discovery, and offers excellent interpretability. (2) HMOE leverages hypernetworks to generate expert weights and achieves sparse-gated MoE. (3) As far as we know, HMOE is the first work that can jointly learn and use latent domains in an end-to-end way. (4) Extensive experiments are conducted to compare HMOE with other DG methods under a fair evaluation framework – DomainBed [28]. HMOE exhibits state-of-the-art performance on most datasets and greatly outperforms other DG methods in average accuracy.

## 2. Related Work

### 2.1. Domain Generalization (DG)

The goal of DG is to train a predictor on known domains that can generalize well to unseen domains.

**Vanilla DG** The first line of work is to design DG-specific data augmentation techniques to increase the diversity and quantity of training data to improve DG performance [51, 65, 70, 84, 91, 93, 98, 100]. Previous work learned domain-invariant representations through invariant risk minimization [1, 2, 41], kernel methods [6, 22, 26, 58], feature alignment [25, 47, 56, 57, 61, 63, 76, 78, 86], and domain-adversarial training [23, 24, 27, 47, 49]. Another approach is to disentangle latent features into class-specific and domain-specific representations [35, 38, 59, 64, 94].

General machine learning paradigms were also applied to vanilla DG, such as meta-learning [3, 17, 45, 46], self-supervised learning [8, 39], gradient manipulation [34, 66, 72], and distributionally robust optimization [41, 67].

**Compound DG** There are some DG algorithms that do not require domain labels by design [11, 34, 48, 56, 59, 94]. Besides improving DG performance, latent domain discovery is also an important task for compound DG and contributes to better interpretability. [11, 56] can do this but have two main limitations: (1) Their methods proceed in two phases: first infer latent domains from mixed data and then deal with DG using the inferred domains, which is similar to vanilla DG. The problem is that the second phase depends on the first and cannot provide some feedback to correct possible errors in domain discovery. (2) Their methods assume that domain shift arises from stylistic differences to identify latent domains, which does not always hold.

On the contrary, HMOE is trained in an end-to-end manner and leverages MoE to discover latent domains without an explicit induced bias on the cause of domain shift.

### 2.2. Hypernetworks

A hypernetwork is a neural network that generates the weights of another target network. Hypernetworks were initially proposed by [30] and have since been applied to optimization problems [53, 60], meta-learning [96], continuous learning [7, 85], multi-task learning [50, 54, 77], few-shot learning [68], and federated learning [69].

### 2.3. Mixture of Experts (MoE)

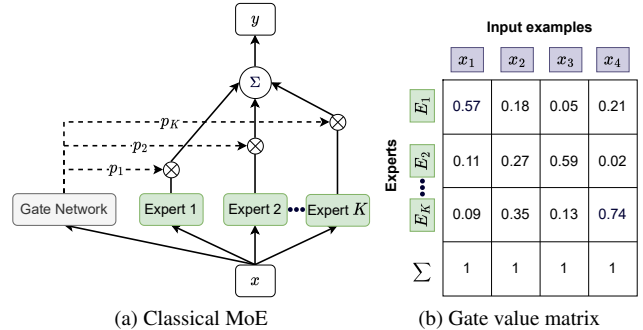


Figure 1. (a) MoE calculates the weighted sum of experts' outputs. (b) Gate values are determined by a gate network.

MoE was originally proposed by [36, 37] and consists of two main components: experts and a gate network, as shown in Fig. 1. The output of MoE is the weighted sum of experts, with gate values calculated by the gate network on a per-example basis. In recent years, MoE has regained attention as a way to scale up deep learning models and more efficiently harness modern hardware [18, 20, 21, 42, 71, 102]. In this case, sparse MoE is preferred, which routes each example only to the experts with Top-1 or Top-K gate values.

## 2.4. Application of Hypernetworks and MoE in DG

As far as we know, no work has applied hypernetworks to solve DG in computer vision. Recently, [83] applied hypernetworks to DG in natural language processing (NLP) and achieved SOTA results on two NLP-related DG tasks.

As for MoE, [43] proposed replacing feed-forward network layer (FFN) of Vision Transformer (ViT) [16] with a sparse mixture of FFN experts to improve DG performance. [29, 97] applied MoE to a task similar to DG, namely domain adaptation [88], but they require domain labels to train an expert for each domain separately. [97] aggregates the outputs of experts via a transformer-based aggregator, but its aggregator is trained with fixed experts and cannot provide probabilities of experts, while HMOE can do this and is more interpretable. In addition, if we regard MoE as a kind of ensemble method, [15, 55, 99] share the same spirit.

## 3. Method

### 3.1. Problem Setting

Let  $\mathcal{X}$  denote an input space and  $\mathcal{Y}$  a target space. A domain  $S$  is characterized by a joint distribution  $P_{XY}^s$  on  $\mathcal{X} \times \mathcal{Y}$ . In vanilla DG setting, we have a training set containing  $M$  known domains, *i.e.*,  $\mathcal{D}_{tr}^V = \{\mathcal{D}^s\}_{s=1}^M$  with  $\mathcal{D}^s = \{(x_i^s, y_i^s, d_i^s)\}_{i=1}^{N_s}$  where  $(x_i^s, y_i^s) \sim P_{XY}^s$  and  $d_i^s$  is the domain index or label. Also consider a test dataset  $\mathcal{D}_{te}$  composed of unknown domains different from those of  $\mathcal{D}_{tr}^V$ . Vanilla DG aims to train a robust predictor  $f : \mathcal{X} \rightarrow \mathcal{Y}$  on  $\mathcal{D}_{tr}^V$  to achieve a minimum predictive error on  $\mathcal{D}_{te}$ , *i.e.*,  $\min_f \mathbb{E}_{(x,y) \sim \mathcal{D}_{te}} [\ell(f(x), y)]$ , where  $\ell$  is the loss function.

Our work focuses on the more difficult compound DG, for which the training set  $\mathcal{D}_{tr} = \{(x_i, y_i)\}_{i=1}^N$  contains mixed domains and has no domain annotation. However, as demonstrated in [28, 87, 101], intrinsic inter-domain relationships play a key role in obtaining better generalization performance. Therefore, our proposed HMOE is designed to discover latent domains by dividing  $\mathcal{D}_{tr}$  into clusters and to fully leverage the learned domain information in order to perform well on unknown domains.

### 3.2. Overall Architecture

An overview of HMOE is illustrated in Fig. 2a. HMOE processes input  $x$  through two paths: the domain path for latent domain discovery and the classifier path to train an expert for each latent domain.

The classifier path begins with a featurizer  $h_z$  to extract high-level features from  $x$ , which can be a pretrained network, such as VGG [74], ResNet [32], or ViT [16]. We define a discrete learnable embedding space  $\mathcal{E}$  consisting of  $K$  embedding vectors  $\{e_k \in \mathbb{R}^D\}_{k=1}^K$  ( $D$  represents the embedding dimension), each corresponding to a classifier expert. These vectors are fed into a hypernetwork  $f_h$  to generate a set of weights  $\{\theta_k\}_{k=1}^K$ , which further form a set

of experts  $\{f_c(\cdot; \theta_k)\}_{k=1}^K$ . The output of the featurizer  $z$  is passed to these experts to compute their corresponding outputs, that is,  $y_k = f_c(z; \theta_k)$ .

The domain path begins with a Domain2Vec (D2V) encoder  $h_v$ , which transforms  $x$  into the embedding space  $\mathcal{E}$  and outputs  $v \in \mathbb{R}^D$ . The output  $v$  is then compared with the embedding vectors through a predefined gate function  $g(v, \mathcal{E})$ , as shown in Fig. 2b, to produce a set of probabilities  $\mathbf{p} = \{p_k\}_{k=1}^K$ . The final output of HMOE is the weighted sum of the outputs of experts as follows:

$$y = \sum_{k=1}^K p_k y_k = g(h_v(x), \mathcal{E}) \cdot [f_c(h_z(x); f_h(e_k))]_{k=1}^K \quad (1)$$

### 3.3. Hypernetworks

We employ a hypernetwork  $f_h$  taking a vector  $e$  as input to produce weights for classifier  $f_c$ . In our work, both  $f_h$  and  $f_c$  are MLPs. Essentially,  $f_c$  acts as a computational graph placeholder,  $e$  is a conditioning signal, and  $f_h$  maps  $e$  to a function. The roles of  $f_h$  include: (1) easing latent domain discovery, (2) using many experts without a major increase in parameters, (3) offering another interaction between experts and the routing mechanism besides the aggregation of experts compared to the classical MoE, and (4) enabling the generalization of experts beyond aggregation (As we will see later,  $f_h$  can directly take the D2V encoder as input).

### 3.4. Routing Mechanism

#### 3.4.1 Gate Function

To quantify the responsibilities of experts for each input example and to aggregate experts' outputs, we need to calculate gate values  $\mathbf{p}$ . As shown in Fig. 2b, based on the output of the D2V encoder  $v$  and the embedding space  $\mathcal{E}$ , we define a gate function  $g(v, \mathcal{E})$  to calculate  $\mathbf{p}$  as follows:

$$d_k = \|v - e_k\|_2 \quad (2a)$$

$$s_k = -\log(d_k^2 + \epsilon) \quad (2b)$$

$$p_k = \frac{\exp(s_k)}{\sum_{j=1}^K \exp(s_j)} \quad (2c)$$

where  $\epsilon$  is a small value. The negative logarithm in Eq. (2b) is used to establish a negative correlation between  $d_k$  and  $p_k$  (*i.e.*, the smaller  $d_k$ , the larger  $p_k$ ) and to nonlinearly rescale the distance  $d$  (*i.e.*, stretch small  $d$  and squeeze great  $d$ ), which makes  $\mathbf{p}$  less sensitive to large  $d$ .

#### 3.4.2 Differentiable Dense-to-Sparse Top-1 Routing

Based on gate values  $\mathbf{p}$ , the routing mechanism determines where and how to route input examples. A consistent and cohesive routing is crucial to the training stability and convergence of MoE [12]. In order to stabilize the routing and

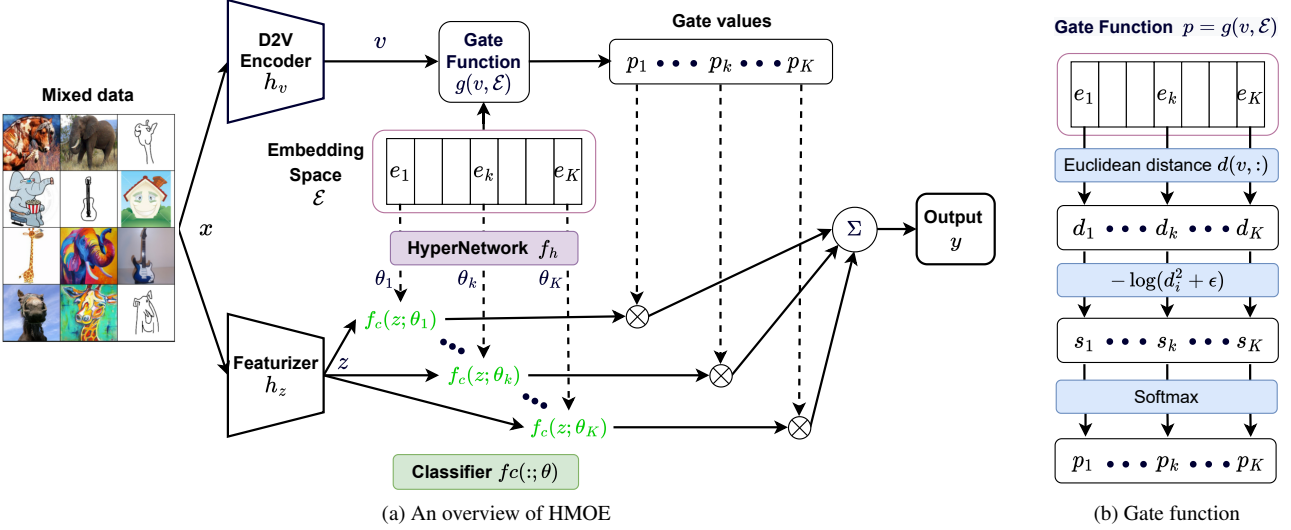


Figure 2. (a) In the upper branch (*i.e.*, the domain path), the input goes through the D2V encoder into the embedding space, and a predefined gate function calculates gate values. In the lower branch (*i.e.*, the classifier path), the hypernetwork takes the embedding vectors as input to create a set of classifiers. The final output is the weighted sum of the outputs of classifiers. (b) The gate function determines gate values based on the distances between the output of the D2V encoder and embedding vectors. Smaller distances yield greater gate values.

enhance latent domain discovery to capture less obvious domain differences, sparse-gated MoE is preferable. However, the commonly used Top-1 or Top-K functions are not differentiable and may cause oscillatory behavior of gate values during training [31]. To overcome this limitation, we propose a differentiable dense-to-sparse Top-1 routing algorithm by introducing an entropy loss on  $\mathbf{p}$  as follows:

$$\mathcal{L}_{en} = \mathbb{E}_{(x,y) \sim \mathcal{D}_{tr}} [\mathbb{H}(g(h_v(x), \mathcal{E}))] \quad (3)$$

where  $\mathbb{H}(\cdot)$  denotes the entropy of a distribution. In practice, we multiply  $\mathcal{L}_{en}$  by  $\gamma_{en}$  that linearly increases from 0 to 1 in the first half of training and remains at 1 in the second. Early on,  $\gamma_{en}$  is small, and the distances between  $v$  and the embedding vectors are almost the same, leading to a uniform  $\mathbf{p}$ . Therefore, all experts can be fully trained and gradually become specialized. In the later stages,  $\mathcal{L}_{en}$  forces  $\mathbf{p}$  to become one-hot based on specialized experts.

Due to the negative logarithm in Eq. (2b), the D2V encoder has to move towards one embedding vector to minimize  $\mathcal{L}_{en}$  instead of moving away from others.

### 3.4.3 Expert Load Balancing

Sparse-gated MoE may suffer from an unbalanced expert load. We define the importance of experts as  $I(X) = [I_1(X), \dots, I_K(X)]$ , where  $X$  represents a single batch and  $I_k(X)$  is specified as the sum of gate values assigned to the  $k$ th expert (*i.e.*, sum the gate value matrix in Fig. 1b along the example dimension). [62] defines a distribution  $P = I(X) / \sum I(X)$  and uses the KL-divergence between

$P$  and the uniform distribution  $\mathcal{U}$  to balance the expert load, which is also used in our work:

$$L_{kl} = D_{KL}(P || \mathcal{U}) = D_{KL}\left(\frac{I(X)}{\sum I(X)} || \mathcal{U}\right) \quad (4)$$

### 3.5. Embedding Space

The embedding space  $\mathcal{E}$  plays a key role in HMOE. As we can see, the embedding vectors have an effect on both the generation of expert weights and the routing mechanism, thus serving as a bridge to balance these two parts. In addition, these embedding vectors are learnable like the weights of neural networks and attract the D2V encoder during training under the influence of  $\mathcal{L}_{en}$ .

### 3.6. Class-Adversarial Training on D2V

We expect the D2V encoder  $h_v$  to contain as little class-specific information as possible, which ensures that HMOE partitions the input space based on domain-wise distinction rather than semantic categories. Inspired by Domain-Adversarial Neural Networks [24], we define an adversarial classifier  $f_c^{ad}$  taking  $v$  as input and add the following loss to perform class-adversarial training on  $h_v$ :

$$\mathcal{L}_{ad} = \mathbb{E}_{(x,y) \sim \mathcal{D}_{tr}} [\ell_{ce}(f_c^{ad}(GRL(v, \lambda_{grl})), y)] \quad (5)$$

where  $\ell_{ce}$  denotes the cross-entropy loss and  $GRL$  represents the gradient reversal layer, which acts as an identity function in the forward pass and multiplies the gradient by  $-\lambda_{grl}$  in the backward pass. As suggested in [24], we define  $\lambda_{grl}$  as follows:

$$\lambda_{grl} = 2 / (1 + \exp(-10 \times pct_{tr})) - 1 \quad (6)$$

where  $pct_{tr}$  varies linearly from 0 to 1 during training.

### 3.7. Supervised Learning on Targets

We provide two ways to calculate the supervised loss on targets  $\mathcal{L}_y$ , that is, Empirical Risk Minimization (ERM) [81] and the intra-domain *mixup*.

**ERM** In the setting of ERM, the supervised loss on targets is simply the empirical risk on the training data  $\mathcal{D}_{tr}$ :

$$\mathcal{L}_y = \mathbb{E}_{(x,y) \sim \mathcal{D}_{tr}} [\ell_{ce}(\hat{y}, y)] \quad (7)$$

where  $\hat{y}$  is the prediction of HMOE, as calculated by Eq. (1).

**Intra-domain mixup** *mixup* trains a neural network on virtual samples synthesized through convex combinations of pairs of samples and their labels [93]:

$$\tilde{x} = \beta x_i + (1 - \beta)x_j \quad (8)$$

$$\tilde{y} = \beta y_i + (1 - \beta)y_j \quad (9)$$

where  $\beta \sim \text{Beta}(\alpha, \alpha)$  and  $\alpha$  adjusts interpolation strength. *mixup* can be seen as a data augmentation approach theoretically grounded in Vicinal Risk Minimization [10], which is an alternative learning principle to ERM. [89, 90] applied the inter-domain *mixup* mixing samples across different domains for domain-invariant learning, whereas our intra-domain *mixup*, as shown in Algorithm 1, prompts HMOE for smoother predictions in neighborhood within each domain, enhancing its generalization and robustness.

To perform the intra-domain *mixup* without domain labels, HMOE starts with Eq. (7) and then switches to Algorithm 1 until  $\mathcal{L}_{en} < 0.1$  indicating latent domains are reasonably discovered and clustered.

---

#### Algorithm 1 intra-domain *mixup*

**Require:** A mini-batch  $\mathcal{B}$  split into distinct domains given domain labels or clusters identified by gate values

- 1: **for each** domain or cluster  $\mathcal{B}_i \in \mathcal{B}$  **do**
- 2:      $\tilde{\mathcal{B}}_i \leftarrow \text{mixup}(\mathcal{B}_i, \text{shuffled } \mathcal{B}_i)$  with  $\beta \sim \text{Beta}(\alpha, \alpha)$   
    ▷ Mix same-index samples between  $\mathcal{B}_i$  and shuffled  $\mathcal{B}_i$
- 3:     Compute the empirical risk  $\mathcal{L}_i$  on  $\tilde{\mathcal{B}}_i$
- 4: **end for**
- 5:  $\mathcal{L}_y \leftarrow \text{Average over all } \mathcal{L}_i$

---

### 3.8. Semi-/supervised Learning on Domains

Due to the probabilistic nature of MoE, given an input  $x$  and the corresponding gate values  $\mathbf{p} = \{p_k\}_{k=1}^K$ , we can interpret  $p_k$  as the probability of selecting the  $k$ th expert  $E_k$  given  $x$ , *i.e.*,  $p(E_k|x)$ . In addition,  $E_k$  is thought to be associated with a specific domain  $\mathcal{S}_m$ . Therefore, we get  $p_k = p(E_k|x) = p(\mathcal{S}_m|x)$ . Consider a dataset with domain labels  $\mathcal{D}_d = \{(x_i, d_i)\}_{i=1}^{N_d}$  (class labels are not necessary) with  $d_i \in \{1, \dots, M_d\}$ , we can make use of  $\mathcal{D}_d$  as follows:

$$\mathcal{L}_d = \mathbb{E}_{(x,d) \sim \mathcal{D}_d} [\ell_{ce}(\mathbf{p}, d)] \quad (10)$$

$M_d$  may be smaller than  $K$ , but this has no bearing on the calculation of  $\mathcal{L}_d$ . In this case, we assume that the first  $M_d$  experts are assigned to  $M_d$  domains, while the rest learn autonomously without domain information. If all domain labels are given,  $\mathcal{L}_d$  shifts to supervised domain learning.

### 3.9. Training and Inference

The final training loss is:

$$\mathcal{L} = \lambda_y \mathcal{L}_y + \lambda_{en} \mathcal{L}_{en} + \lambda_{kl} \mathcal{L}_{kl} + \lambda_{ad} \mathcal{L}_{ad} + \lambda_d \mathcal{L}_d \quad (11)$$

where  $\lambda$  are trade-off hyper-parameters to balance different losses. Generally,  $\lambda_y$  is set to 1 and  $\mathcal{L}_d$  is not used for compound DG without domain labels.

For inference, we offer two modes: MIX and OOD. MIX refers to the mixture of experts, as calculated by Eq. (1). OOD<sup>1</sup> (Out of Domain) uses the output of a classifier whose weights are generated by the hypernetwork directly taking the D2V encoder as input. OOD enables the generalization of experts beyond aggregation.

## 4. Experiments

This paper focuses on image classification. However, to illustrate HMOE’s learning dynamics and versatility, we also apply it to a toy regression task to learn a one-dimensional function defined on 3 intervals. HMOE proves effective in assigning an expert to each interval. Due to space limits, details are in the **supplementary material**. Next, we evaluate HMOE against other DG algorithms on DomainBed [28].

### 4.1. Datasets and Model Evaluation

DomainBed offers a unified codebase to implement, train, and evaluate DG algorithms, and integrates commonly used DG-related datasets. We experiment on Colored MNIST (3 domains and 2 classes) [2], Rotated MNIST (6 domains and 10 classes) [25], PACS (4 domains and 7 classes) [44], VLCS (4 domains and 5 classes) [19], OfficeHome (4 domains and 65 classes) [82], and TerraIncognita (4 domains and 10 classes) [4]. Detailed dataset statistics and sample visualization are provided in the **supplementary material**.

For model selection and hyper-parameter tuning, DomainBed offers three options, of which we choose the training-domain validation that allocates 80% from each training domain for training and the rest for validation. This option aligns well with compound DG without access to domain labels and test domains.

### 4.2. Implementation Details

For CMNIST and RMNIST, we use a four-layer ConvNet as the featurizer (see Appendix D.1 of [28]). The D2V encoder  $h_v$  connects this four-layer ConvNet to a fully-connected (fc) layer in order to map to the embedding dimension  $D$ .

<sup>1</sup>OOD is efficiently realized using PyTorch-based JAX-like *functorch*.

For other datasets, we use ResNet-50 pretrained on ImageNet [13] as the featurizer and freeze all batch normalization layers. The D2V encoder  $h_v$  cascades 3 *conv* layers (64-128-256 units, stride 2,  $4 \times 4$  kernels, ReLU), two residual blocks (each has 2 *conv* layers with 256 units,  $3 \times 3$  kernels, ReLU), and a  $3 \times 3$  *conv* layer with  $D$  units followed by global average pooling. We use Instance Normalization [79] with learnable affine parameters before all ReLU of  $h_v$ .

For all datasets, the classifier  $f_c$  is a fc layer whose input size is the featurizer’s output size (128 for ConvNet and 2048 for ResNet-50) and output size is the number of classes. The hypernetwork  $f_h$  is a five-layer MLP with 256-128-64-32 hidden units and SiLU [33], and its input size is  $D$  and output size is the total number of learnable parameters (*i.e.*, weights and biases) of  $f_c$ . In addition, we initialize  $f_h$  using the hyperfan method [9]. If  $\mathcal{L}_{ad}$  is used, the adversarial classifier is a three-layer MLP with 256 hidden units and ReLU, and its input size is  $D$  and output size is the number of classes. We set  $D = 32$  and initialize embedding vectors with the standard normal distribution.

We define three HMOE variants, including (1) **HMOE-DL**: Domain labels are provided. We use  $\mathcal{L}_y$  calculated by Eq. (7) and  $\mathcal{L}_d$  with  $\lambda_y = \lambda_d = 1$  and discard other losses, and  $K$  is the number of training domains. (2) **HMOE-ND**: No domain information is available. We use  $\mathcal{L}_y$  calculated by Eq. (7),  $\mathcal{L}_{en}$ ,  $\mathcal{L}_{kl}$  and  $\mathcal{L}_{ad}$  with  $\lambda_y = \lambda_{en} = \lambda_{kl} = 1$  and  $\lambda_{ad} = 0.1$ , and we fix  $K = 3$ . (3) **HMOE-MU**: The setting is the same as in HMOE-ND, except that  $\mathcal{L}_y$  is calculated via the intra-domain *mixup* (Algorithm 1) with  $\alpha = 0.3$ .

DomainBed trains all DG algorithms with Adam for 5,000 iterations. For Colored and Rotated MNIST / other datasets, the learning rate is 0.001 / 5e-5, the batch size is  $64 / 32 \times$  the number of training domains, and models are evaluated on the validation set every 100 / 300 iterations. Each experiment uses one domain of a dataset as the test domain and trains algorithms on the others, which is repeated three times with different random seeds. The average accuracy over three replicates is reported. DG algorithms use the default settings predefined in DomainBed. All experiments are conducted using PyTorch on multiple A5000 GPUs.

### 4.3. Results

The DomainBed benchmark in [28] has been outdated, and we update it using an improved pretrained ResNet-50 (IMAGENET1K-V2) available on torchvision. The comparison of HMOE against other DG algorithms is shown in Tab. 1, where DeepAll means the vanilla supervised learning that just fine-tunes ResNet-50 on mixed data and serves as a performance baseline. We report the average accuracy of all test domains for each dataset. Refer to the **supplementary material** for detailed results.

HMOE-MU outperforms all other DG algorithms in average accuracy. Notably, *mixup*-powered algorithms show

impressive performance, proving the effectiveness of *mixup* in enhancing generalization. Both Mixup [90] (second place) and SelfReg [39] (third place) adopted the inter-domain *mixup* to learn domain-invariant representations. HMOE-ND ranks fourth overall, but is the top among algorithms without *mixup*. In addition, HMOE-ND / MU largely surpass the DeepAll baseline, except on RMNIST.

For MNIST datasets, performance is comparable across algorithms, except for the outstanding results of ARM [95]. Other datasets pose higher challenges. For instance, VLCS comprises real photo images, with the domain shift primarily caused by changes in scene and perspective, leading to subtle visual differences between domains. Many algorithms are inferior to DeepAll on these challenging datasets. HMOE-MU achieves state-of-the-art results on PACS, OfficeHome, and TerraInc, and its performance on VLCS is nearly on par with the best result (78.6 vs. 78.9). HMOE-ND also performs impressively. All these findings validate the superiority of HMOE in addressing compound DG.

HMOE-MU markedly surpasses ND. Fig. 3a presents a comparison of their validation / test accuracy during training. It is evident that the accuracy of MU continues to improve with the introduction of intra-domain *mixup* upon  $\mathcal{L}_{en} < 0.1$ , because *mixup* imposes linearity constraints, which prompts smoothness and mitigates overfitting.

Interestingly, HMOE-DL lags behind HMOE-ND / MU significantly, indicating that HMOE performs better when using self-learned domain information rather than relying on provided domain labels. We observe that the latent domains discovered by HMOE seem to be more human-intuitive than given domain labels (Sec. 4.4). Fig. 3b shows that the supervised loss on domains  $\mathcal{L}_d$  of HMOE-DL fails to decrease rapidly on OfficeHome and VLCS datasets. This could suggest that HMOE struggles to assimilate domain label information, which complicates its learning process and negatively affects its DG performance.

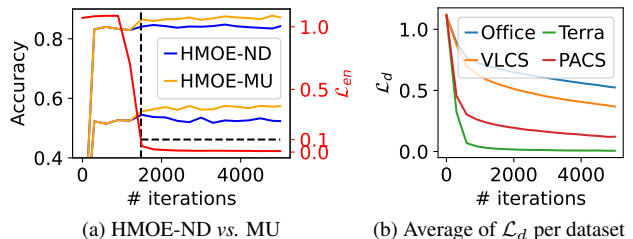


Figure 3. Losses over iterations. (a) ND / MU on OfficeHome with *clipart* as the test domain. The upper / lower curves of ND / MU represent their validation / test accuracy, respectively.

For two inference modes, MIX outperforms OOD in most cases, but OOD can be used to sacrifice a little accuracy for efficiency in practice because it is more computationally efficient without computing all experts like MIX.

Algorithm	M	CMNIST	RMNIST	VLCS	PACS	OfficeHome	TerraInc	Avg	Ranking
<i>w/ Domain Labels</i>									
Mixup [90]	✓	51.9 ± 0.1	97.6 ± 0.1	78.7 ± 0.1	86.6 ± 0.1	71.6 ± 0.2	51.4 ± 0.4	72.97	2
CORAL [76]		51.4 ± 0.1	98.0 ± 0.0	78.1 ± 0.2	86.7 ± 0.4	72.2 ± 0.2	48.9 ± 0.5	72.55	5
VREx [41]		52.2 ± 0.1	97.8 ± 0.0	77.3 ± 0.2	86.0 ± 0.7	69.8 ± 0.1	51.8 ± 0.4	72.48	6
Fish [73]		51.5 ± 0.1	97.9 ± 0.1	78.1 ± 0.0	86.9 ± 0.9	68.7 ± 0.1	51.0 ± 0.7	72.35	7
ARM [95]		55.6 ± 0.3	98.1 ± 0.0	78.0 ± 0.6	85.7 ± 0.8	66.5 ± 0.4	48.5 ± 0.4	72.05	9
MTL [6]		51.5 ± 0.2	97.8 ± 0.0	77.3 ± 0.3	85.5 ± 0.2	68.4 ± 0.5	51.3 ± 0.6	71.97	10
GroupDRO [67]		52.1 ± 0.0	97.8 ± 0.0	77.8 ± 0.6	85.0 ± 0.8	68.3 ± 0.3	49.6 ± 0.5	71.77	11
MLDG [45]		44.2 ± 4.6	97.8 ± 0.0	76.6 ± 0.2	87.1 ± 0.1	68.3 ± 0.3	49.9 ± 1.1	70.65	15
MMD [47]		38.5 ± 0.8	98.0 ± 0.0	77.4 ± 0.9	84.2 ± 0.1	69.1 ± 0.0	50.0 ± 1.2	69.53	16
DANN [24]		51.8 ± 0.1	97.7 ± 0.0	75.6 ± 0.6	77.0 ± 1.4	66.5 ± 0.3	42.5 ± 2.6	68.52	17
IRM [2]		41.3 ± 0.9	87.3 ± 0.4	78.3 ± 1.1	82.1 ± 0.7	64.9 ± 0.3	50.8 ± 1.1	67.45	18
HMOE-DL	MIX	51.5 ± 0.1	94.1 ± 0.5	77.0 ± 0.4	85.5 ± 0.6	68.9 ± 0.6	49.6 ± 0.2	71.70	14
	OOD	57.0 ± 3.9	93.3 ± 0.5	77.9 ± 0.3	85.1 ± 0.8	67.9 ± 0.3	48.3 ± 0.4	71.58	
<i>w/o Domain Labels</i>									
SelfReg [39]	✓	51.4 ± 0.1	98.0 ± 0.0	78.9 ± 0.3	86.1 ± 0.3	71.3 ± 0.2	51.5 ± 0.3	72.87	3
SagNet [59]		51.8 ± 0.1	98.0 ± 0.0	77.7 ± 0.3	86.2 ± 0.4	69.3 ± 0.2	50.7 ± 0.5	72.28	8
RSC [34]		51.5 ± 0.2	97.5 ± 0.1	78.8 ± 0.3	87.0 ± 0.4	65.5 ± 0.9	49.1 ± 1.0	71.57	12
DeepAll [81]		51.4 ± 0.1	97.8 ± 0.1	77.5 ± 0.2	85.8 ± 0.4	68.5 ± 0.2	47.7 ± 0.9	71.45	13
HMOE-ND	MIX	51.8 ± 0.1	97.5 ± 0.1	78.1 ± 0.3	86.6 ± 0.3	69.7 ± 0.2	52.5 ± 0.3	72.70	4
	OOD	51.8 ± 0.1	97.5 ± 0.1	78.0 ± 0.4	86.9 ± 0.2	69.0 ± 0.2	51.1 ± 1.4	72.38	
HMOE-MU	✓	MIX	51.7 ± 0.2	97.6 ± 0.1	78.6 ± 0.0	88.0 ± 0.3	72.5 ± 0.1	52.8 ± 0.9	73.53
	OOD	51.6 ± 0.2	97.6 ± 0.1	78.8 ± 0.3	87.0 ± 1.0	72.4 ± 0.1	52.1 ± 0.9	73.25	1

Table 1. Domain generalization results on DomainBed. We format *first*, *second* and *worse* than DeepAll results. *M* denotes the inter/intra-*mixup*. The performance of HMOE is evidenced by MIX. OOD is only for comparison with MIX and does not participate in the ranking.

#### 4.4. Latent Domain Discovery

We employ t-SNE [80] to visualize the output of the D2V encoder, as shown in Fig. 4. It is evident that HMOE-ND effectively separates the mixed data into distinct clusters, each gravitating towards an embedding vector.

Domain labels are used to color data to highlight the differences between them and inferred latent domains. For PACS with the *art* test (Fig. 4a), inferred domains largely align with domain labels, although some photos are grouped into the cartoon-predominant cluster. However, with *cartoon* as the test domain (Fig. 4b), data is not split based on *art* and *photo*. Fig. 4e shows that, even with domain labels, HMOE-DL struggles to fully separate *art* from *photo*. For TerraInc (Fig. 4c), points of the same color tend to cluster together, whereas for OfficeHome (Fig. 4d), different colors intermix within each cluster, highlighting the big gap between labeled and inferred domains. Fig. 4f also shows that HMOE-DL has difficulty in data partitioning, explaining the slow decrease in  $\mathcal{L}_d$  for OfficeHome in Fig. 3b.

To intuitively understand how HMOE distinguishes between domains, Fig. 5 compares labeled and inferred domains using visual samples. HMOE-ND seems to partition TerraInc by illumination and OfficeHome by background complexity, which aligns more with human intuition.

After the above analysis, we conclude that the success of HMOE stems from its ability to self-learn more reasonable

domain knowledge. However, this does not mean that given domain labels are erroneous. There are typically multiple generative factors behind the data-generating process [5], rendering the definition of domains multifaceted. HMOE simply discovers an intuitive and digestible way of data partitioning in order to enhance its DG performance.

#### 4.5. Ablation Studies

The role of the intra-domain *mixup* has been validated before. In this section, we analyze the contribution of other components of HMOE through ablation studies, as shown in Tab. 2. We use the silhouette coefficient (SC) to quantitatively evaluate the clustering of HMOE in terms of cluster compactness and separation. SC ranges from -1 (poor) to 1 (good). Clusters are identified by gate values and their distances are measured using the output of the D2V encoder.

Name	$\mathcal{L}_{en}$	$\mathcal{L}_{kl}$	$\mathcal{L}_{ad}$	VLCS	PACS	Office	TerraInc	Avg.	SC
H1	-	-	-	78.0	86.8	68.4	50.5	0.37	
H2	-	-	✓	77.8	<b>86.9</b>	69.1	51.2	0.27	
H3	✓	-	-	77.3	84.8	69.0	48.2	Collapse	
H4	✓	-	✓	77.8	86.3	68.6	49.2	Collapse	
H5	✓	✓	-	77.7	86.8	68.7	50.5	0.65	
H6	✓	✓	✓	<b>78.1</b>	86.6	<b>69.7</b>	<b>52.5</b>	0.60	

Table 2. Ablation studies for HMOE-ND (✓ means the corresponding loss is used and SC denotes the silhouette coefficient.)

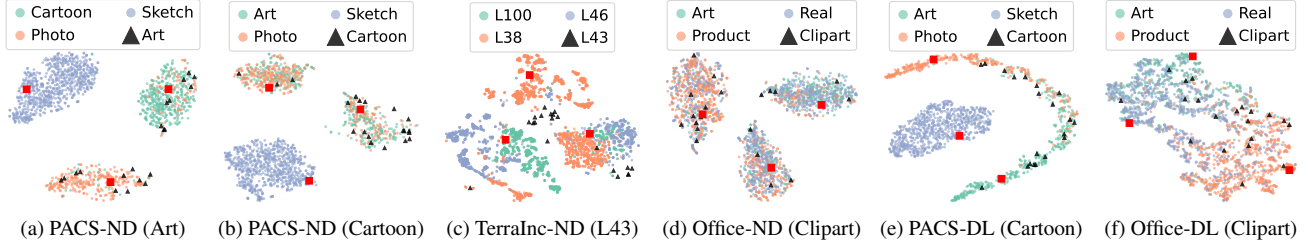


Figure 4. The t-SNE visualization of the output of the D2V encoder. The suffixes in captions denote HMOE-DL / ND, with the test domain in parentheses. Red squares are embedding vectors, black triangles are 20 samples randomly drawn from the test domain, and other dots are training domains. The silhouette coefficients are 0.7, 0.68, 0.48, 0.66, 0.46, and 0.36 for Figs. 4a to 4f, respectively.

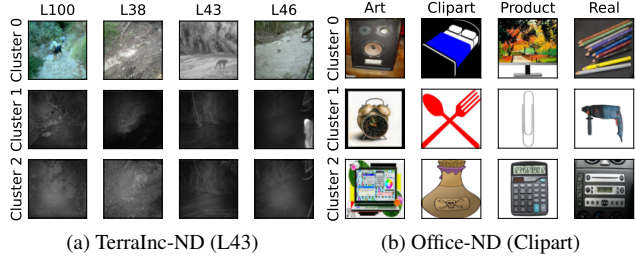


Figure 5. Compare domain labels and HMOE-ND clusters

#### Top-1 routing $\mathcal{L}_{en}$ and expert load balancing $\mathcal{L}_{kl}$

The joint use of  $\mathcal{L}_{en}$  and  $\mathcal{L}_{kl}$  leads to better clustering with greater SC and promotes latent domain discovery. Without them, HMOE relies on the inherent soft partitioning of MoE. H6 outperforms H2 mostly, which could indicate that better clustering benefits DG performance. However, H1 and H5 perform similarly, probably due to the absence of  $\mathcal{L}_{ad}$ . We find that  $\mathcal{L}_{en}$  without  $\mathcal{L}_{kl}$  suffers from the learning collapse problem, *i.e.*, some embedding vectors collapse together, leading to a drop in accuracy. An example is shown in Fig. 6c. This demonstrates the importance of  $\mathcal{L}_{kl}$ .

**Class-adversarial training**  $\mathcal{L}_{ad}$  boosts accuracy in most cases, verifying the necessity of filtering out class-specific information from the D2V encoder. H2 and H6 have smaller SC than H1 and H5, respectively, which is reasonable since class information can still be used by H1 and H5 for clustering, but is somewhat diminished for H2 and H6 via  $\mathcal{L}_{ad}$ .

#### 4.6. More Empirical Analysis

**Effect of  $K$  on latent domain discovery** In Fig. 6, we try different numbers of embedding vectors  $K$ . For  $K = 2$ , *cartoon* is merged into *sketch* and *photo*. For  $K = 5$ , *sketch* and *cartoon* are split into two sub-clusters. However, when  $K$  increases to 8 and is much more than necessary, HMOE has difficulty in assigning data to different experts correctly and suffers from the learning collapse problem.

**Use Swin Transformer as featurizer** [43] investigated the impact of the backbone network (*i.e.*, the featurizer for HMOE) on DG and found that transformer-based back-

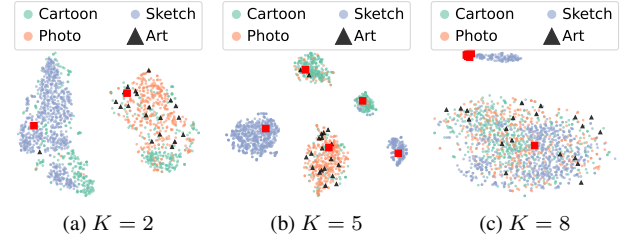


Figure 6. HMOE-ND using different  $K$  for PACS (Art)

bones outperform CNN-based counterparts. Motivated by this, we try Swin Transformer [52] (pretrained tiny version with similar complexity to ResNet-50 and its output size is 768) as featurizer (Tab. 3), which enhances both DeepAll and HMOE-MU, but the latter still performs much better.

	VLCS	PACS	OfficeHome	TerraInc
DeepAll	79.7	86.5	71.9	52.9
HMOE-MU	79.8	88.1	74.6	54.7

Table 3. Use Swin Transformer as featurizer of HMOE

## 5. Conclusion

This paper presents a novel DG method – HMOE, which is based on Mixture of Experts, uses hypernetworks to generate the weights of experts, does not require domain labels, and enables latent domain discovery. HMOE achieves the SOTA performance in average accuracy on DomainBed.

However, it remains unclear how to effectively determine an appropriate number of experts or embedding vectors to fully explore domain information while avoiding the learning collapse. A promising solution that we will explore in future work is to use tree-structured hierarchical MoE to discover hierarchical domain knowledge, where each level contains only a number of experts but the number of multi-level inferred domains grows exponentially.

Finally, HMOE is versatile and scalable, and it should also be applicable to a wide range of problems beyond the scope of DG that are troubled by heterogeneous patterns.

# HMOE: Hypernetwork-based Mixture of Experts for Domain Generalization

## Supplementary Material

### A. Toy Regression Problem

In the paper, we employ HMOE to address the domain generalization problem in image classification. In fact, HMOE is equally applicable to other problems troubled by heterogeneous patterns. To demonstrate the versatility of HMOE, we apply it to a toy regression task, aiming to learn a one-dimensional function defined over three intervals. Through this toy problem, we can also more intuitively understand the learning dynamics of HMOE, including the evolution of the gating mechanism and how experts become specialized gradually.

We use the function  $y = \sin(4\pi x)$  to generate 10, 20, and 30 data points uniformly in three intervals:  $(0, 0.5)$ ,  $(1, 1.5)$ , and  $(2, 2.5)$ , respectively, as shown in Fig. 7a. Unequal data points are used to simulate a naturally unbalanced expert load. These three intervals represent three source domains, and we see if HMOE can generalize well in the regions between intervals.

HMOE uses three embedding vectors of dimension  $D = 8$ , which are initialized using the standard normal distribution. All networks of HMOE are MLPs with 32 hidden units. The featurizer is a three-layer MLP whose input size is 1 and output size is 32. The encoder is a three-layer whose input size is 1 and output size is  $D$ . The classifier is a two-layer MLP whose input size is 32 and output size is 1. The hypernetwork is a four-layer MLP whose input size is  $D$  and output size is the total number of learnable parameters (*i.e.*, weights and biases) of the classifier. All MLPs use the SiLU activation function [33] except the output layers. In addition,  $\mathcal{L}_y$  (use MSE as the loss function),  $\mathcal{L}_{en}$ , and  $\mathcal{L}_{kl}$  are used with  $\lambda_y = \lambda_{en} = \lambda_{kl} = 1$ , and HMOE is trained using Adam [40] with learning rate 0.001 over 20,000 epochs.

The evolution of the experts' outputs and gate values with respect to training epochs is depicted in Fig. 7a. From this, we can observe that three experts compete with each other and progressively delineate their respective positions. Notably, HMOE manages to identify three intervals even in the face of imbalanced data. After training, we compare two different inference modes, as shown in Fig. 7b. They all coincide well with the training points. MIX seems to perform better in the regions between intervals, while OOD presents an unexpected peak. Overall, HMOE demonstrates an ability to detect heterogeneous patterns within data.

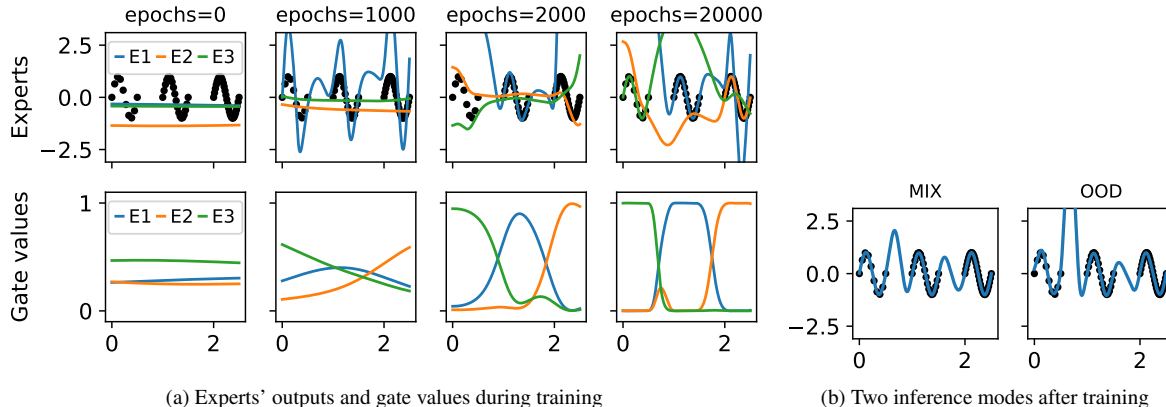


Figure 7. A toy regression problem. We generate some data points using the function  $y = \sin(4\pi x)$  in three intervals and fit HMOE with three embedding vectors to these points. HMOE well identifies three intervals and experts also become specialized.

## B. Description and visualization of datasets of DomainBed

Dataset	Domains			# of classes	# of samples	Image size
Colored MNIST [2]	+90%	+80%	-90%			
	<i>(degree of correlation between color and label)</i>					
Rotated MNIST [25]	0°	15°	30°	45°	60°	75°
VLCS [19]	Caltech101	LabelMe	SUN09	VOC2007		
PACS [44]	Art	Cartoon	Photo	Sketch		
OfficeHome [82]	Clipart	Product	Photo			
TerraIncognita [4]	L100	L38	L43	L46		
	<i>(camera trap location)</i>					

Table 4. Description and visualization of datasets used in our experiments (Adapted from [28])

## C. Detailed domain generalization results

We detail the domain generalization results for each dataset, and we format first, second and worse than DeepAll results.

Algorithm	+90%	+80%	-90%	Avg	Ranking
<i>w/ Domain Labels</i>					
Mixup [90]	$72.3 \pm 0.1$	$73.1 \pm 0.0$	$10.4 \pm 0.1$	51.9	4
CORAL [76]	$71.3 \pm 0.3$	$73.0 \pm 0.2$	$9.9 \pm 0.0$	51.4	13
VREx [41]	<u><math>73.1 \pm 0.3</math></u>	<u><math>73.7 \pm 0.3</math></u>	$10.0 \pm 0.1$	<u>52.2</u>	2
Fish [73]	$71.3 \pm 0.1$	$73.1 \pm 0.2$	$10.2 \pm 0.1$	51.5	9
ARM [95]	<u><math>81.7 \pm 0.5</math></u>	<u><math>74.8 \pm 1.1</math></u>	$10.3 \pm 0.2$	<u>55.6</u>	1
MTL [6]	$71.6 \pm 0.3$	$72.9 \pm 0.3$	$10.2 \pm 0.0$	51.5	10
GroupDRO [67]	$73.0 \pm 0.1$	$73.0 \pm 0.4$	$10.2 \pm 0.3$	52.1	3
MLDG [45]	$37.5 \pm 9.9$	$56.4 \pm 5.2$	<u><math>38.8 \pm 8.1</math></u>	44.2	16
MMD [47]	$53.9 \pm 2.7$	$51.6 \pm 0.8$	$10.1 \pm 0.1$	38.5	18
DANN [24]	$72.5 \pm 0.1$	$72.7 \pm 0.2$	$10.1 \pm 0.1$	51.8	5
IRM [2]	$57.0 \pm 2.7$	$57.2 \pm 4.9$	$9.7 \pm 0.0$	41.3	17
HMOE-DL	$71.5 \pm 0.4$	$72.9 \pm 0.1$	$10.2 \pm 0.0$	51.5	11
<i>w/o Domain Labels</i>					
SelfReg [39]	$71.1 \pm 0.3$	$73.0 \pm 0.0$	$10.1 \pm 0.2$	51.4	14
SagNet [59]	$72.2 \pm 0.0$	$73.3 \pm 0.3$	$10.0 \pm 0.1$	51.8	6
RSC [34]	$72.1 \pm 0.3$	$72.3 \pm 0.8$	$10.1 \pm 0.1$	51.5	12
DeepAll [81]	$71.6 \pm 0.1$	$72.7 \pm 0.2$	$10.0 \pm 0.1$	51.4	15
HMOE-ND	$71.8 \pm 0.1$	$73.0 \pm 0.1$	$10.5 \pm 0.2$	51.8	7
HMOE-MU	$71.7 \pm 0.4$	$73.0 \pm 0.3$	$10.3 \pm 0.1$	51.7	8

Table 5. Domain generalization results on Colored MNIST

Algorithm	0	15	30	45	60	75	Avg	Ranking
<i>w/ Domain Labels</i>								
Mixup [90]	93.8 $\pm$ 0.1	98.8 $\pm$ 0.1	99.0 $\pm$ 0.0	99.1 $\pm$ 0.1	98.9 $\pm$ 0.0	95.9 $\pm$ 0.2	97.6	13
CORAL [76]	95.8 $\pm$ 0.2	98.5 $\pm$ 0.1	99.1 $\pm$ 0.0	99.0 $\pm$ 0.1	99.1 $\pm$ 0.0	96.6 $\pm$ 0.1	98.0	2
VREx [41]	95.5 $\pm$ 0.1	98.3 $\pm$ 0.2	98.9 $\pm$ 0.1	98.9 $\pm$ 0.0	98.9 $\pm$ 0.0	96.4 $\pm$ 0.1	97.8	7
Fish [73]	95.5 $\pm$ 0.4	98.7 $\pm$ 0.0	99.0 $\pm$ 0.0	99.1 $\pm$ 0.1	98.9 $\pm$ 0.0	96.3 $\pm$ 0.3	97.9	6
ARM [95]	95.9 $\pm$ 0.1	98.8 $\pm$ 0.0	98.9 $\pm$ 0.1	99.1 $\pm$ 0.0	98.9 $\pm$ 0.0	96.2 $\pm$ 0.1	98.1	1
MTL [6]	95.2 $\pm$ 0.2	98.6 $\pm$ 0.1	99.1 $\pm$ 0.0	98.9 $\pm$ 0.1	98.8 $\pm$ 0.1	96.1 $\pm$ 0.1	97.8	8
GroupDRO [67]	94.9 $\pm$ 0.2	98.6 $\pm$ 0.1	98.9 $\pm$ 0.0	99.0 $\pm$ 0.1	99.0 $\pm$ 0.0	96.3 $\pm$ 0.1	97.8	9
MLDG [45]	95.3 $\pm$ 0.1	98.5 $\pm$ 0.1	99.0 $\pm$ 0.0	99.0 $\pm$ 0.0	98.9 $\pm$ 0.1	96.1 $\pm$ 0.1	97.8	10
MMD [47]	95.8 $\pm$ 0.3	98.8 $\pm$ 0.0	99.0 $\pm$ 0.1	98.9 $\pm$ 0.0	99.0 $\pm$ 0.0	96.2 $\pm$ 0.1	98.0	3
DANN [24]	95.9 $\pm$ 0.1	98.5 $\pm$ 0.1	98.6 $\pm$ 0.0	98.8 $\pm$ 0.0	98.7 $\pm$ 0.0	95.6 $\pm$ 0.1	97.7	12
IRM [2]	81.9 $\pm$ 2.4	88.1 $\pm$ 4.2	93.2 $\pm$ 0.6	91.3 $\pm$ 2.8	93.1 $\pm$ 0.7	76.0 $\pm$ 0.7	87.3	18
HMOE-DL	87.7 $\pm$ 1.3	93.3 $\pm$ 2.2	98.2 $\pm$ 0.3	98.6 $\pm$ 0.0	98.2 $\pm$ 0.2	88.8 $\pm$ 1.5	94.1	17
<i>w/o Domain Labels</i>								
SelfReg [39]	95.7 $\pm$ 0.1	98.7 $\pm$ 0.0	99.0 $\pm$ 0.0	99.2 $\pm$ 0.0	99.1 $\pm$ 0.0	96.5 $\pm$ 0.1	98.0	4
SagNet [59]	95.1 $\pm$ 0.3	98.8 $\pm$ 0.0	99.1 $\pm$ 0.0	99.1 $\pm$ 0.1	99.0 $\pm$ 0.0	96.7 $\pm$ 0.1	98.0	5
RSC [34]	94.0 $\pm$ 0.3	98.3 $\pm$ 0.1	99.0 $\pm$ 0.0	98.9 $\pm$ 0.0	98.9 $\pm$ 0.0	95.9 $\pm$ 0.1	97.5	15
DeepAll [81]	95.0 $\pm$ 0.4	98.5 $\pm$ 0.2	99.0 $\pm$ 0.0	99.1 $\pm$ 0.0	98.9 $\pm$ 0.0	96.2 $\pm$ 0.1	97.8	11
HMOE-ND	94.5 $\pm$ 0.1	98.5 $\pm$ 0.1	98.8 $\pm$ 0.0	98.7 $\pm$ 0.0	98.7 $\pm$ 0.1	95.7 $\pm$ 0.3	97.5	16
HMOE-MU	94.6 $\pm$ 0.3	98.8 $\pm$ 0.0	98.9 $\pm$ 0.1	98.8 $\pm$ 0.0	98.8 $\pm$ 0.1	95.6 $\pm$ 0.2	97.6	14

Table 6. Domain generalization results on Rotated MNIST

Algorithm	Caltech101	LabelMe	SUN09	VOC2007	Avg	Ranking
<i>w/ Domain Labels</i>						
Mixup [90]	98.2 $\pm$ 0.3	64.8 $\pm$ 0.3	74.9 $\pm$ 0.2	76.9 $\pm$ 1.0	78.7	3
CORAL [76]	97.2 $\pm$ 0.4	65.8 $\pm$ 0.4	74.0 $\pm$ 0.3	75.4 $\pm$ 0.8	78.1	6
VREx [41]	96.1 $\pm$ 0.5	64.8 $\pm$ 1.2	72.6 $\pm$ 0.5	75.5 $\pm$ 1.0	77.3	14
Fish [73]	96.8 $\pm$ 0.5	64.5 $\pm$ 0.3	74.9 $\pm$ 0.3	76.1 $\pm$ 1.0	78.1	7
ARM [95]	97.0 $\pm$ 0.2	65.9 $\pm$ 1.4	73.0 $\pm$ 0.1	76.2 $\pm$ 1.4	78.0	9
MTL [6]	96.3 $\pm$ 0.1	64.5 $\pm$ 0.3	72.6 $\pm$ 0.5	75.6 $\pm$ 0.9	77.3	15
GroupDRO [67]	97.1 $\pm$ 0.3	65.9 $\pm$ 0.7	72.4 $\pm$ 1.7	75.8 $\pm$ 0.4	77.8	10
MLDG [45]	96.9 $\pm$ 0.6	61.5 $\pm$ 0.8	71.7 $\pm$ 0.7	76.5 $\pm$ 0.2	76.6	17
MMD [47]	96.9 $\pm$ 0.5	64.2 $\pm$ 1.9	71.7 $\pm$ 0.9	76.6 $\pm$ 1.8	77.4	13
DANN [24]	95.8 $\pm$ 1.0	65.1 $\pm$ 0.7	68.1 $\pm$ 2.4	73.5 $\pm$ 0.7	75.6	18
IRM [2]	96.8 $\pm$ 0.3	64.6 $\pm$ 1.2	75.2 $\pm$ 0.8	76.6 $\pm$ 3.4	78.3	5
HMOE-DL	95.5 $\pm$ 1.4	63.5 $\pm$ 0.5	73.8 $\pm$ 1.0	75.0 $\pm$ 1.5	77.0	16
<i>w/o Domain Labels</i>						
SelfReg [39]	97.6 $\pm$ 0.4	65.2 $\pm$ 0.2	75.5 $\pm$ 0.2	77.1 $\pm$ 0.7	78.9	1
SagNet [59]	96.8 $\pm$ 0.1	63.0 $\pm$ 1.0	72.3 $\pm$ 0.2	78.7 $\pm$ 1.1	77.7	11
RSC [34]	96.7 $\pm$ 0.9	64.7 $\pm$ 0.7	76.4 $\pm$ 0.6	77.4 $\pm$ 0.8	78.8	2
DeepAll [81]	95.0 $\pm$ 0.5	65.4 $\pm$ 1.0	72.0 $\pm$ 1.2	77.7 $\pm$ 0.3	77.5	12
HMOE-ND	96.8 $\pm$ 0.5	64.7 $\pm$ 0.5	75.0 $\pm$ 0.1	76.1 $\pm$ 1.5	78.1	8
HMOE-MU	97.1 $\pm$ 0.2	64.6 $\pm$ 0.7	74.9 $\pm$ 0.4	77.9 $\pm$ 0.3	78.6	4

Table 7. Domain generalization results on VLCS

Algorithm	Art	Cartoon	Photo	Sketch	Avg	Ranking
<i>w/ Domain Labels</i>						
Mixup [90]	88.1 $\pm$ 0.3	81.7 $\pm$ 1.0	98.1 $\pm$ 0.1	78.6 $\pm$ 1.6	86.6	6
CORAL [76]	87.8 $\pm$ 0.9	82.7 $\pm$ 0.9	98.0 $\pm$ 0.1	78.4 $\pm$ 1.8	86.7	5
VREx [41]	86.5 $\pm$ 2.0	79.2 $\pm$ 0.9	97.7 $\pm$ 0.3	80.6 $\pm$ 1.2	86.0	10
Fish [73]	86.0 $\pm$ 1.8	83.1 $\pm$ 0.3	98.1 $\pm$ 0.3	80.5 $\pm$ 2.3	86.9	4
ARM [95]	86.2 $\pm$ 1.2	81.5 $\pm$ 0.7	97.2 $\pm$ 0.3	77.9 $\pm$ 1.1	85.7	12
MTL [6]	88.4 $\pm$ 0.8	80.7 $\pm$ 1.2	97.8 $\pm$ 0.2	75.2 $\pm$ 1.8	85.5	13
GroupDRO [67]	86.3 $\pm$ 1.9	81.0 $\pm$ 0.6	97.8 $\pm$ 0.1	74.9 $\pm$ 2.0	85.0	15
MLDG [45]	90.7 $\pm$ 0.3	80.4 $\pm$ 0.4	97.9 $\pm$ 0.1	79.5 $\pm$ 0.8	87.1	2
MMD [47]	87.0 $\pm$ 0.4	79.6 $\pm$ 0.9	97.4 $\pm$ 0.3	72.6 $\pm$ 1.8	84.2	16
DANN [24]	79.4 $\pm$ 1.9	74.7 $\pm$ 0.9	97.0 $\pm$ 1.1	57.1 $\pm$ 7.0	77.0	18
IRM [2]	84.8 $\pm$ 1.8	73.9 $\pm$ 1.9	98.6 $\pm$ 0.1	71.3 $\pm$ 1.0	82.1	17
HMOE-DL	87.5 $\pm$ 1.4	78.9 $\pm$ 1.3	97.6 $\pm$ 0.1	77.9 $\pm$ 1.3	85.5	14
<i>w/o Domain Labels</i>						
SelfReg [39]	86.8 $\pm$ 2.0	82.3 $\pm$ 0.8	97.6 $\pm$ 0.2	77.8 $\pm$ 0.8	86.1	9
SagNet [59]	85.3 $\pm$ 2.0	81.8 $\pm$ 1.6	97.7 $\pm$ 0.3	79.8 $\pm$ 0.8	86.2	8
RSC [34]	86.6 $\pm$ 1.2	82.4 $\pm$ 0.4	97.4 $\pm$ 0.3	81.6 $\pm$ 0.7	87.0	3
DeepAll [81]	86.4 $\pm$ 1.2	81.7 $\pm$ 0.6	97.5 $\pm$ 0.3	77.7 $\pm$ 1.8	85.8	11
HMOE-ND	87.1 $\pm$ 0.7	81.7 $\pm$ 0.9	97.7 $\pm$ 0.1	79.9 $\pm$ 1.1	86.6	7
HMOE-MU	89.6 $\pm$ 0.5	81.2 $\pm$ 1.0	98.3 $\pm$ 0.2	82.9 $\pm$ 1.6	88.0	1

Table 8. Domain generalization results on PACS

Algorithm	Art	Clipart	Product	Real	Avg	Ranking
<i>w/ Domain Labels</i>						
Mixup [90]	68.1 $\pm$ 0.8	55.9 $\pm$ 0.8	80.3 $\pm$ 0.1	82.0 $\pm$ 0.3	71.6	3
CORAL [76]	69.9 $\pm$ 0.7	56.8 $\pm$ 0.1	80.5 $\pm$ 0.4	81.7 $\pm$ 0.2	72.2	2
VREx [41]	66.4 $\pm$ 0.8	54.0 $\pm$ 0.4	78.2 $\pm$ 0.2	80.6 $\pm$ 0.2	69.8	5
Fish [73]	64.3 $\pm$ 0.3	53.0 $\pm$ 0.4	78.1 $\pm$ 0.1	79.4 $\pm$ 0.7	68.7	10
ARM [95]	60.4 $\pm$ 0.2	52.2 $\pm$ 0.6	75.6 $\pm$ 0.6	77.9 $\pm$ 0.3	66.5	15
MTL [6]	64.3 $\pm$ 0.7	52.1 $\pm$ 1.3	78.5 $\pm$ 0.1	78.6 $\pm$ 0.1	68.4	12
GroupDRO [67]	63.7 $\pm$ 0.8	52.9 $\pm$ 0.8	77.6 $\pm$ 0.2	78.8 $\pm$ 0.3	68.3	13
MLDG [45]	64.2 $\pm$ 0.8	52.7 $\pm$ 0.9	78.4 $\pm$ 0.8	78.1 $\pm$ 0.2	68.3	14
MMD [47]	65.6 $\pm$ 0.3	53.7 $\pm$ 0.5	77.8 $\pm$ 0.1	79.4 $\pm$ 0.1	69.1	8
DANN [24]	62.0 $\pm$ 0.9	49.7 $\pm$ 1.8	76.1 $\pm$ 0.5	78.2 $\pm$ 0.4	66.5	16
IRM [2]	60.4 $\pm$ 0.4	49.6 $\pm$ 1.0	73.2 $\pm$ 0.8	76.2 $\pm$ 0.5	64.9	18
HMOE-DL	64.8 $\pm$ 0.7	53.0 $\pm$ 1.4	78.6 $\pm$ 0.3	79.0 $\pm$ 0.3	68.9	9
<i>w/o Domain Labels</i>						
SelfReg [39]	68.0 $\pm$ 0.4	55.7 $\pm$ 0.4	79.7 $\pm$ 0.2	81.9 $\pm$ 0.6	71.3	4
SagNet [59]	63.7 $\pm$ 0.9	54.6 $\pm$ 0.2	78.2 $\pm$ 0.2	80.7 $\pm$ 0.4	69.3	7
RSC [34]	60.7 $\pm$ 1.4	51.4 $\pm$ 0.3	74.8 $\pm$ 1.1	75.1 $\pm$ 1.3	65.5	17
DeepAll [81]	64.7 $\pm$ 0.6	52.2 $\pm$ 1.0	77.4 $\pm$ 0.2	79.8 $\pm$ 0.2	68.5	11
HMOE-ND	65.6 $\pm$ 0.1	54.7 $\pm$ 0.6	78.8 $\pm$ 0.2	79.9 $\pm$ 0.3	69.7	6
HMOE-MU	68.7 $\pm$ 0.6	57.7 $\pm$ 0.4	81.0 $\pm$ 0.2	82.6 $\pm$ 0.4	72.5	1

Table 9. Domain generalization results on OfficeHome

Algorithm	L100	L38	L43	L46	Avg	Ranking
<i>w/ Domain Labels</i>						
Mixup [90]	<b>68.3</b> $\pm$ 2.0	43.9 $\pm$ 0.4	56.9 $\pm$ 1.5	36.6 $\pm$ 0.5	51.4	5
CORAL [76]	52.9 $\pm$ 3.7	46.8 $\pm$ 1.4	59.5 $\pm$ 0.4	36.3 $\pm$ 0.9	48.9	15
VREx [41]	60.7 $\pm$ 1.7	44.8 $\pm$ 1.2	58.9 $\pm$ 1.4	42.6 $\pm$ 1.3	51.8	3
Fish [73]	55.7 $\pm$ 2.2	46.9 $\pm$ 2.5	<b>59.9</b> $\pm$ 0.4	41.3 $\pm$ 2.1	51.0	7
ARM [95]	56.0 $\pm$ 3.1	44.3 $\pm$ 1.4	54.9 $\pm$ 0.3	38.6 $\pm$ 0.6	48.5	16
MTL [6]	55.1 $\pm$ 0.8	<b>51.3</b> $\pm$ 2.3	57.8 $\pm$ 0.8	41.2 $\pm$ 2.1	51.3	6
GroupDRO [67]	51.9 $\pm$ 2.9	45.4 $\pm$ 1.8	<b>60.8</b> $\pm$ 0.7	40.2 $\pm$ 0.3	49.6	12
MLDG [45]	57.6 $\pm$ 3.3	46.2 $\pm$ 1.2	58.4 $\pm$ 0.7	37.5 $\pm$ 0.8	49.9	11
MMD [47]	61.0 $\pm$ 2.7	43.2 $\pm$ 0.6	57.5 $\pm$ 1.5	38.3 $\pm$ 2.2	50.0	10
DANN [24]	48.8 $\pm$ 1.1	38.1 $\pm$ 3.9	44.1 $\pm$ 4.4	38.9 $\pm$ 2.4	42.5	18
IRM [2]	49.4 $\pm$ 4.3	47.6 $\pm$ 2.4	58.4 $\pm$ 1.6	<b>47.8</b> $\pm$ 1.5	50.8	8
HMOE-DL	<b>56.1</b> $\pm$ 1.9	<b>48.1</b> $\pm$ 1.2	<b>57.7</b> $\pm$ 0.8	<b>36.5</b> $\pm$ 1.3	<b>49.6</b>	13
<i>w/o Domain Labels</i>						
SelfReg [39]	59.0 $\pm$ 2.4	46.0 $\pm$ 1.1	59.6 $\pm$ 1.7	41.5 $\pm$ 1.1	51.5	4
SagNet [59]	59.6 $\pm$ 1.3	46.3 $\pm$ 1.1	<b>59.8</b> $\pm$ 0.7	37.2 $\pm$ 1.6	50.7	9
RSC [34]	51.7 $\pm$ 6.4	46.4 $\pm$ 0.7	59.1 $\pm$ 0.9	39.2 $\pm$ 1.1	49.1	14
DeepAll [81]	50.0 $\pm$ 3.4	42.3 $\pm$ 1.6	<b>58.5</b> $\pm$ 1.0	39.9 $\pm$ 2.3	47.7	17
HMOE-ND	<b>60.7</b> $\pm$ 3.6	<b>53.2</b> $\pm$ 1.5	<b>56.7</b> $\pm$ 1.2	<b>39.6</b> $\pm$ 0.3	<b>52.5</b>	<b>2</b>
HMOE-MU	67.3 $\pm$ 1.0	43.4 $\pm$ 1.4	57.4 $\pm$ 0.7	<b>43.0</b> $\pm$ 2.8	<b>52.8</b>	<b>1</b>

Table 10. Domain generalization results on TerraInc

## References

- [1] Kartik Ahuja, Ethan Caballero, Dinghuai Zhang, Jean-Christophe Gagnon-Audet, Yoshua Bengio, Ioannis Mitliagkas, and Irina Rish. Invariance principle meets information bottleneck for out-of-distribution generalization. *Advances in Neural Information Processing Systems*, 34:3438–3450, 2021. [2](#)
- [2] Martin Arjovsky, Léon Bottou, Ishaaan Gulrajani, and David Lopez-Paz. Invariant risk minimization. *arXiv preprint arXiv:1907.02893*, 2019. [2, 5, 7, 3, 4](#)
- [3] Yogesh Balaji, Swami Sankaranarayanan, and Rama Chellappa. Metareg: Towards domain generalization using meta-regularization. *Advances in neural information processing systems*, 31, 2018. [2](#)
- [4] Sara Beery, Grant Van Horn, and Pietro Perona. Recognition in terra incognita. In *Proceedings of the European Conference on Computer Vision (ECCV)*, pages 456–473, 2018. [5, 2](#)
- [5] Yoshua Bengio, Aaron Courville, and Pascal Vincent. Representation learning: A review and new perspectives. *IEEE transactions on pattern analysis and machine intelligence*, 35(8):1798–1828, 2013. [7](#)
- [6] Gilles Blanchard, Aniket Anand Deshmukh, Ürun Dogan, Gyemin Lee, and Clayton Scott. Domain generalization by marginal transfer learning. *The Journal of Machine Learning Research*, 22(1):46–100, 2021. [1, 2, 7, 3, 4, 5](#)
- [7] Dhanajit Brahma, Vinay Kumar Verma, and Piyush Rai. Hypernetworks for Continual Semi-Supervised Learning. *arXiv preprint arXiv:2110.01856*, 2021. [2](#)
- [8] Fabio M. Carlucci, Antonio D’Innocente, Silvia Bucci, Barbara Caputo, and Tatiana Tommasi. Domain generalization by solving jigsaw puzzles. In *Proceedings of the IEEE/CVF Conference on Computer Vision and Pattern Recognition*, pages 2229–2238, 2019. [2](#)
- [9] Oscar Chang, Lampros Flokas, and Hod Lipson. Principled weight initialization for hypernetworks. In *International Conference on Learning Representations*, 2019. [6](#)
- [10] Olivier Chapelle, Jason Weston, Léon Bottou, and Vladimir Vapnik. Vicinal risk minimization. *Advances in neural information processing systems*, 13, 2000. [5](#)
- [11] Chaoqi Chen, Jiongcheng Li, Xiaoguang Han, Xiaoqing Liu, and Yizhou Yu. Compound Domain Generalization via Meta-Knowledge Encoding. In *Proceedings of the IEEE/CVF Conference on Computer Vision and Pattern Recognition*, pages 7119–7129, 2022. [1, 2](#)
- [12] Damai Dai, Li Dong, Shuming Ma, Bo Zheng, Zhifang Sui, Baobao Chang, and Furu Wei. StableMoE: Stable routing strategy for mixture of experts. *arXiv preprint arXiv:2204.08396*, 2022. [3](#)
- [13] Jia Deng, Wei Dong, Richard Socher, Li-Jia Li, Kai Li, and Li Fei-Fei. Imagenet: A large-scale hierarchical image database. In *2009 IEEE Conference on Computer Vision and Pattern Recognition*, pages 248–255. Ieee, 2009. [6](#)
- [14] Aniket Anand Deshmukh, Yunwen Lei, Srinagesh Sharma, Urur Dogan, James W. Cutler, and Clayton Scott. A generalization error bound for multi-class domain generalization. *arXiv preprint arXiv:1905.10392*, 2019. [1](#)
- [15] Antonio D’Innocente and Barbara Caputo. Domain generalization with domain-specific aggregation modules. In *German Conference on Pattern Recognition*, pages 187–198. Springer, 2018. [3](#)
- [16] Alexey Dosovitskiy, Lucas Beyer, Alexander Kolesnikov, Dirk Weissenborn, Xiaohua Zhai, Thomas Unterthiner, Mostafa Dehghani, Matthias Minderer, Georg Heigold, and Sylvain Gelly. An image is worth 16x16 words: Transformers for image recognition at scale. *arXiv preprint arXiv:2010.11929*, 2020. [3](#)
- [17] Qi Dou, Daniel Coelho de Castro, Konstantinos Kamnitsas, and Ben Glocker. Domain generalization via model-agnostic learning of semantic features. *Advances in Neural Information Processing Systems*, 32, 2019. [2](#)
- [18] Nan Du, Yanping Huang, Andrew M. Dai, Simon Tong, Dmitry Lepikhin, Yuanzhong Xu, Maxim Krikun, Yanqi Zhou, Adams Wei Yu, and Orhan Firat. Glam: Efficient scaling of language models with mixture-of-experts. In *International Conference on Machine Learning*, pages 5547–5569. PMLR, 2022. [2](#)
- [19] Chen Fang, Ye Xu, and Daniel N. Rockmore. Unbiased metric learning: On the utilization of multiple datasets and web images for softening bias. In *Proceedings of the IEEE International Conference on Computer Vision*, pages 1657–1664, 2013. [5, 2](#)
- [20] William Fedus, Barret Zoph, and Noam Shazeer. *Switch Transformers: Scaling to Trillion Parameter Models with Simple and Efficient Sparsity*. 2021. [2](#)
- [21] William Fedus, Jeff Dean, and Barret Zoph. A review of sparse expert models in deep learning. *arXiv preprint arXiv:2209.01667*, 2022. [2](#)
- [22] Chuang Gan, Tianbao Yang, and Boqing Gong. Learning attributes equals multi-source domain generalization. In *Proceedings of the IEEE Conference on Computer Vision and Pattern Recognition*, pages 87–97, 2016. [2](#)
- [23] Yaroslav Ganin and Victor Lempitsky. Unsupervised domain adaptation by backpropagation. In *International Conference on Machine Learning*, pages 1180–1189. PMLR, 2015. [2](#)
- [24] Yaroslav Ganin, Evgeniya Ustinova, Hana Ajakan, Pascal Germain, Hugo Larochelle, François Laviolette, Mario Marchand, and Victor Lempitsky. Domain-adversarial training of neural networks. *The journal of machine learning research*, 17(1):2096–2030, 2016. [2, 4, 7, 3, 5](#)

[25] Muhammad Ghifary, W. Bastiaan Kleijn, Mengjie Zhang, and David Balduzzi. Domain generalization for object recognition with multi-task autoencoders. In *Proceedings of the IEEE International Conference on Computer Vision*, pages 2551–2559, 2015. [2](#) [5](#)

[26] Muhammad Ghifary, David Balduzzi, W. Bastiaan Kleijn, and Mengjie Zhang. Scatter component analysis: A unified framework for domain adaptation and domain generalization. *IEEE transactions on pattern analysis and machine intelligence*, 39(7):1414–1430, 2016. [2](#)

[27] Rui Gong, Wen Li, Yuhua Chen, and Luc Van Gool. Dlow: Domain flow for adaptation and generalization. In *Proceedings of the IEEE/CVF Conference on Computer Vision and Pattern Recognition*, pages 2477–2486, 2019. [2](#)

[28] Ishaan Gulrajani and David Lopez-Paz. In search of lost domain generalization. *arXiv preprint arXiv:2007.01434*, 2020. [1](#), [2](#), [3](#), [5](#), [6](#)

[29] Jiang Guo, Darsh J. Shah, and Regina Barzilay. Multi-source domain adaptation with mixture of experts. *arXiv preprint arXiv:1809.02256*, 2018. [1](#), [3](#)

[30] David Ha, Andrew Dai, and Quoc V. Le. Hypernetworks. *arXiv preprint arXiv:1609.09106*, 2016. [1](#), [2](#)

[31] Hussein Hazimeh, Zhe Zhao, Aakanksha Chowdhery, Maheswaran Sathiamoorthy, Yihua Chen, Rahul Mazumder, Lichan Hong, and Ed Chi. Dselect-k: Differentiable selection in the mixture of experts with applications to multi-task learning. *Advances in Neural Information Processing Systems*, 34:29335–29347, 2021. [4](#)

[32] Kaiming He, Xiangyu Zhang, Shaoqing Ren, and Jian Sun. Deep residual learning for image recognition. In *Proceedings of the IEEE Conference on Computer Vision and Pattern Recognition*, pages 770–778, 2016. [3](#)

[33] Dan Hendrycks and Kevin Gimpel. Gaussian error linear units (gelus). *arXiv preprint arXiv:1606.08415*, 2016. [6](#), [1](#)

[34] Zeyi Huang, Haohan Wang, Eric P. Xing, and Dong Huang. Self-challenging improves cross-domain generalization. In *European Conference on Computer Vision*, pages 124–140. Springer, 2020. [2](#), [7](#), [3](#), [4](#), [5](#)

[35] Maximilian Ilse, Jakub M Tomczak, Christos Louizos, and Max Welling. Diva: Domain invariant variational autoencoders. In *Medical Imaging with Deep Learning*, pages 322–348. PMLR, 2020. [2](#)

[36] Robert A. Jacobs, Michael I. Jordan, Steven J. Nowlan, and Geoffrey E. Hinton. Adaptive mixtures of local experts. *Neural computation*, 3(1):79–87, 1991. [1](#), [2](#)

[37] Michael I. Jordan and Robert A. Jacobs. Hierarchical mixtures of experts and the EM algorithm. *Neural computation*, 6(2):181–214, 1994. [1](#), [2](#)

[38] Aditya Khosla, Tinghui Zhou, Tomasz Malisiewicz, Alexei A. Efros, and Antonio Torralba. Undoing the damage of dataset bias. In *European Conference on Computer Vision*, pages 158–171. Springer, 2012. [2](#)

[39] Daehye Kim, Youngjun Yoo, Seunghyun Park, Jinkyu Kim, and Jaekoo Lee. Selfreg: Self-supervised contrastive regularization for domain generalization. In *Proceedings of the IEEE/CVF International Conference on Computer Vision*, pages 9619–9628, 2021. [2](#), [6](#), [7](#), [3](#), [4](#), [5](#)

[40] Diederik P Kingma and Jimmy Ba. Adam: A method for stochastic optimization. *arXiv preprint arXiv:1412.6980*, 2014. [1](#)

[41] David Krueger, Ethan Caballero, Joern-Henrik Jacobsen, Amy Zhang, Jonathan Binas, Dinghuai Zhang, Remi Le Priol, and Aaron Courville. Out-of-distribution generalization via risk extrapolation (rex). In *International Conference on Machine Learning*, pages 5815–5826. PMLR, 2021. [2](#), [7](#), [3](#), [4](#), [5](#)

[42] Dmitry Lepikhin, HyoukJoong Lee, Yuanzhong Xu, Dehao Chen, Orhan Firat, Yanping Huang, Maxim Krikun, Noam Shazeer, and Zhifeng Chen. Gshard: Scaling giant models with conditional computation and automatic sharding. *arXiv preprint arXiv:2006.16668*, 2020. [2](#)

[43] Bo Li, Jingkang Yang, Jiawei Ren, Yezhen Wang, and Ziwei Liu. Sparse Fusion Mixture-of-Experts are Domain Generalizable Learners. *arXiv preprint arXiv:2206.04046*, 2022. [3](#), [8](#)

[44] Da Li, Yongxin Yang, Yi-Zhe Song, and Timothy M. Hospedales. Deeper, broader and artier domain generalization. In *Proceedings of the IEEE International Conference on Computer Vision*, pages 5542–5550, 2017. [5](#), [2](#)

[45] Da Li, Yongxin Yang, Yi-Zhe Song, and Timothy Hospedales. Learning to generalize: Meta-learning for domain generalization. In *Proceedings of the AAAI Conference on Artificial Intelligence*, 2018. [2](#), [7](#), [3](#), [4](#), [5](#)

[46] Da Li, Jianshu Zhang, Yongxin Yang, Cong Liu, Yi-Zhe Song, and Timothy M. Hospedales. Episodic training for domain generalization. In *Proceedings of the IEEE/CVF International Conference on Computer Vision*, pages 1446–1455, 2019. [2](#)

[47] Haoliang Li, Sinno Jialin Pan, Shiqi Wang, and Alex C Kot. Domain generalization with adversarial feature learning. In *Proceedings of the IEEE Conference on Computer Vision and Pattern Recognition*, pages 5400–5409, 2018. [2](#), [7](#), [3](#), [4](#), [5](#)

[48] Pan Li, Da Li, Wei Li, Shaogang Gong, Yanwei Fu, and Timothy M. Hospedales. A simple feature augmentation for domain generalization. In *Proceedings of the IEEE/CVF International Conference on Computer Vision*, pages 8886–8895, 2021. [2](#)

[49] Ya Li, Xinmei Tian, Mingming Gong, Yajing Liu, Tongliang Liu, Kun Zhang, and Dacheng Tao. Deep domain generalization via conditional invariant adversarial networks. In *Proceedings of the European Conference on Computer Vision (ECCV)*, pages 624–639, 2018. [2](#)

[50] Xi Lin, Zhiyuan Yang, Qingfu Zhang, and Sam Kwong. Controllable pareto multi-task learning. *arXiv preprint arXiv:2010.06313*, 2020. [2](#)

[51] Alexander H. Liu, Yen-Cheng Liu, Yu-Ying Yeh, and Yu-Chiang Frank Wang. A unified feature disentangler for multi-domain image translation and manipulation. *Advances in neural information processing systems*, 31, 2018. [2](#)

[52] Ze Liu, Yutong Lin, Yue Cao, Han Hu, Yixuan Wei, Zheng Zhang, Stephen Lin, and Baining Guo. Swin transformer: Hierarchical vision transformer using shifted windows. In *Proceedings of the IEEE/CVF International Conference on Computer Vision*, pages 10012–10022, 2021. 8

[53] Jonathan Lorraine and David Duvenaud. Stochastic hyperparameter optimization through hypernetworks. *arXiv preprint arXiv:1802.09419*, 2018. 2

[54] Rabeeh Karimi Mahabadi, Sebastian Ruder, Mostafa Dehghani, and James Henderson. Parameter-efficient multi-task fine-tuning for transformers via shared hypernetworks. *arXiv preprint arXiv:2106.04489*, 2021. 2

[55] Massimiliano Mancini, Samuel Rota Bulo, Barbara Caputo, and Elisa Ricci. Best sources forward: Domain generalization through source-specific nets. In *2018 25th IEEE International Conference on Image Processing (ICIP)*, pages 1353–1357. IEEE, 2018. 3

[56] Toshihiko Matsuura and Tatsuya Harada. Domain generalization using a mixture of multiple latent domains. In *Proceedings of the AAAI Conference on Artificial Intelligence*, pages 11749–11756, 2020. 2

[57] Saeid Motian, Marco Piccirilli, Donald A. Adjeroh, and Gianfranco Doretto. Unified deep supervised domain adaptation and generalization. In *Proceedings of the IEEE International Conference on Computer Vision*, pages 5715–5725, 2017. 2

[58] Krikamol Muandet, David Balduzzi, and Bernhard Schölkopf. Domain generalization via invariant feature representation. In *International Conference on Machine Learning*, pages 10–18. PMLR, 2013. 1, 2

[59] Hyeonseob Nam, HyunJae Lee, Jongchan Park, Wonjun Yoon, and Donggeun Yoo. Reducing domain gap by reducing style bias. In *Proceedings of the IEEE/CVF Conference on Computer Vision and Pattern Recognition*, pages 8690–8699, 2021. 2, 7, 3, 4, 5

[60] Aviv Navon, Aviv Shamsian, Gal Chechik, and Ethan Fetaya. Learning the pareto front with hypernetworks. *arXiv preprint arXiv:2010.04104*, 2020. 2

[61] Sinno Jialin Pan, Ivor W. Tsang, James T. Kwok, and Qiang Yang. Domain adaptation via transfer component analysis. *IEEE transactions on neural networks*, 22(2):199–210, 2010. 2

[62] Svetlana Pavlitskaya, Christian Hubschneider, Lukas Struppek, and J. Marius Zöllner. Balancing Expert Utilization in Mixture-of-Experts Layers Embedded in CNNs. *arXiv preprint arXiv:2204.10598*, 2022. 4

[63] Xingchao Peng, Qinxun Bai, Xide Xia, Zijun Huang, Kate Saenko, and Bo Wang. Moment matching for multi-source domain adaptation. In *Proceedings of the IEEE/CVF International Conference on Computer Vision*, pages 1406–1415, 2019. 2

[64] Xingchao Peng, Zijun Huang, Ximeng Sun, and Kate Saenko. Domain agnostic learning with disentangled representations. In *International Conference on Machine Learning*, pages 5102–5112. PMLR, 2019. 2

[65] Fengchun Qiao, Long Zhao, and Xi Peng. Learning to learn single domain generalization. In *Proceedings of the IEEE/CVF Conference on Computer Vision and Pattern Recognition*, pages 12556–12565, 2020. 2

[66] Alexandre Rame, Corentin Dancette, and Matthieu Cord. Fisher: Invariant gradient variances for out-of-distribution generalization. In *International Conference on Machine Learning*, pages 18347–18377. PMLR, 2022. 2

[67] Shiori Sagawa, Pang Wei Koh, Tatsunori B. Hashimoto, and Percy Liang. Distributionally Robust Neural Networks for Group Shifts: On the Importance of Regularization for Worst-Case Generalization, 2020. 2, 7, 3, 4, 5

[68] Marcin Sendera, Marcin Przewięźlikowski, Konrad Karanowski, Maciej Zieba, Jacek Tabor, and Przemysław Spurek. Hypershot: Few-shot learning by kernel hypernetworks. *arXiv preprint arXiv:2203.11378*, 2022. 2

[69] Aviv Shamsian, Aviv Navon, Ethan Fetaya, and Gal Chechik. Personalized federated learning using hypernetworks. In *International Conference on Machine Learning*, pages 9489–9502. PMLR, 2021. 2

[70] Shiv Shankar, Vihari Piratla, Soumen Chakrabarti, Siddhartha Chaudhuri, Preethi Jyothi, and Sunita Sarawagi. Generalizing across domains via cross-gradient training. *arXiv preprint arXiv:1804.10745*, 2018. 2

[71] Noam Shazeer, Azalia Mirhoseini, Krzysztof Maziarz, Andy Davis, Quoc Le, Geoffrey Hinton, and Jeff Dean. Outrageously large neural networks: The sparsely-gated mixture-of-experts layer. *arXiv preprint arXiv:1701.06538*, 2017. 2

[72] Yuge Shi, Jeffrey Seely, Philip HS Torr, N. Siddharth, Awni Hannun, Nicolas Usunier, and Gabriel Synnaeve. Gradient matching for domain generalization. *arXiv preprint arXiv:2104.09937*, 2021. 2

[73] Yuge Shi, Jeffrey Seely, Philip HS Torr, N Siddharth, Awni Hannun, Nicolas Usunier, and Gabriel Synnaeve. Gradient matching for domain generalization. *arXiv preprint arXiv:2104.09937*, 2021. 7, 2, 3, 4, 5

[74] Karen Simonyan and Andrew Zisserman. Very deep convolutional networks for large-scale image recognition. *arXiv preprint arXiv:1409.1556*, 2014. 3

[75] Trevor Standley, Amir Zamir, Dawn Chen, Leonidas Guibas, Jitendra Malik, and Silvio Savarese. Which tasks should be learned together in multi-task learning? In *International Conference on Machine Learning*, pages 9120–9132. PMLR, 2020. 1

[76] Baochen Sun and Kate Saenko. Deep coral: Correlation alignment for deep domain adaptation. In *European Conference on Computer Vision*, pages 443–450. Springer, 2016. 2, 7, 3, 4, 5

[77] Yi Tay, Zhe Zhao, Dara Bahri, Don Metzler, and Da-Cheng Juan. Hypergrid transformers: Towards a single model for multiple tasks. 2021. 2

[78] Eric Tzeng, Judy Hoffman, Ning Zhang, Kate Saenko, and Trevor Darrell. Deep domain confusion: Maximizing for domain invariance. *arXiv preprint arXiv:1412.3474*, 2014. 2

[79] Dmitry Ulyanov, Andrea Vedaldi, and Victor Lempitsky. Instance normalization: The missing ingredient for fast stylization. *arXiv preprint arXiv:1607.08022*, 2016. 6

[80] Laurens Van der Maaten and Geoffrey Hinton. Visualizing data using t-SNE. *Journal of machine learning research*, 9(11), 2008. 7

[81] Vladimir Vapnik. *The Nature of Statistical Learning Theory*. Springer science & business media, 1999. 5, 7, 2, 3, 4

[82] Hemanth Venkateswara, Jose Eusebio, Shayok Chakraborty, and Sethuraman Panchanathan. Deep hashing network for unsupervised domain adaptation. In *Proceedings of the IEEE Conference on Computer Vision and Pattern Recognition*, pages 5018–5027, 2017. 5, 2

[83] Tomer Volk, Eyal Ben-David, Ohad Amosy, Gal Chechik, and Roi Reichart. Example-based hypernetworks for out-of-distribution generalization. *arXiv preprint arXiv:2203.14276*, 2022. 3

[84] Riccardo Volpi, Hongseok Namkoong, Ozan Sener, John C. Duchi, Vittorio Murino, and Silvio Savarese. Generalizing to unseen domains via adversarial data augmentation. *Advances in neural information processing systems*, 31, 2018. 2

[85] Johannes Von Oswald, Christian Henning, João Sacramento, and Benjamin F. Grewe. Continual learning with hypernetworks. *arXiv preprint arXiv:1906.00695*, 2019. 2

[86] Jindong Wang, Wenjie Feng, Yiqiang Chen, Han Yu, Meiyu Huang, and Philip S. Yu. Visual domain adaptation with manifold embedded distribution alignment. In *Proceedings of the 26th ACM International Conference on Multimedia*, pages 402–410, 2018. 2

[87] Jindong Wang, Cuiling Lan, Chang Liu, Yidong Ouyang, Tao Qin, Wang Lu, Yiqiang Chen, Wenjun Zeng, and Philip Yu. Generalizing to unseen domains: A survey on domain generalization. *IEEE Transactions on Knowledge and Data Engineering*, 2022. 1, 3

[88] Mei Wang and Weihong Deng. Deep visual domain adaptation: A survey. *Neurocomputing*, 312:135–153, 2018. 1, 3

[89] Minghao Xu, Jian Zhang, Bingbing Ni, Teng Li, Chengjie Wang, Qi Tian, and Wenjun Zhang. Adversarial domain adaptation with domain mixup. In *Proceedings of the AAAI conference on artificial intelligence*, pages 6502–6509, 2020. 5

[90] Shen Yan, Huan Song, Nanxiang Li, Lincan Zou, and Liu Ren. Improve unsupervised domain adaptation with mixup training. *arXiv preprint arXiv:2001.00677*, 2020. 5, 6, 7, 2, 3, 4

[91] Xiangyu Yue, Yang Zhang, Sicheng Zhao, Alberto Sangiovanni-Vincentelli, Kurt Keutzer, and Boqing Gong. Domain randomization and pyramid consistency: Simulation-to-real generalization without accessing target domain data. In *Proceedings of the IEEE/CVF International Conference on Computer Vision*, pages 2100–2110, 2019. 2

[92] Seniha Esen Yuksel, Joseph N. Wilson, and Paul D. Gader. Twenty years of mixture of experts. *IEEE transactions on neural networks and learning systems*, 23(8):1177–1193, 2012. 1

[93] Hongyi Zhang, Moustapha Cisse, Yann N Dauphin, and David Lopez-Paz. Mixup: Beyond empirical risk minimization. *arXiv preprint arXiv:1710.09412*, 2017. 2, 5

[94] Hanlin Zhang, Yi-Fan Zhang, Weiyang Liu, Adrian Weller, Bernhard Schölkopf, and Eric P Xing. Towards principled disentanglement for domain generalization. In *Proceedings of the IEEE/CVF Conference on Computer Vision and Pattern Recognition*, pages 8024–8034, 2022. 2

[95] Marvin Zhang, Henrik Marklund, Nikita Dhawan, Abhishek Gupta, Sergey Levine, and Chelsea Finn. Adaptive risk minimization: Learning to adapt to domain shift. *Advances in Neural Information Processing Systems*, 34:23664–23678, 2021. 6, 7, 2, 3, 4, 5

[96] Dominic Zhao, Johannes von Oswald, Seijin Kobayashi, João Sacramento, and Benjamin F. Grewe. Meta-learning via hypernetworks. 2020. 2

[97] Tao Zhong, Zhixiang Chi, Li Gu, Yang Wang, Yuanhao Yu, and Jin Tang. Meta-DMoE: Adapting to Domain Shift by Meta-Distillation from Mixture-of-Experts. *arXiv preprint arXiv:2210.03885*, 2022. 1, 3

[98] Kaiyang Zhou, Yongxin Yang, Timothy Hospedales, and Tao Xiang. Learning to generate novel domains for domain generalization. In *European Conference on Computer Vision*, pages 561–578. Springer, 2020. 2

[99] Kaiyang Zhou, Yongxin Yang, Yu Qiao, and Tao Xiang. Domain adaptive ensemble learning. *IEEE Transactions on Image Processing*, 30:8008–8018, 2021. 3

[100] Kaiyang Zhou, Yongxin Yang, Yu Qiao, and Tao Xiang. Domain generalization with mixstyle. *arXiv preprint arXiv:2104.02008*, 2021. 2

[101] Kaiyang Zhou, Ziwei Liu, Yu Qiao, Tao Xiang, and Chen Change Loy. Domain generalization: A survey. *IEEE Transactions on Pattern Analysis and Machine Intelligence*, 2022. 1, 3

[102] Barret Zoph, Irwan Bello, Sameer Kumar, Nan Du, Yanping Huang, Jeff Dean, Noam Shazeer, and William Fedus. Designing effective sparse expert models. *arXiv preprint arXiv:2202.08906*, 2022. 2